

OBSERVATIONS OF THE OUTBURST OF V694 MON IN 2019.

KONDRATYEVA, L.¹, REVA, I.^{1,2}, KRUGOV, M.¹, AIMANOVA, G.¹, NIZOVKINA, M.^{1,2}, OMAR, B.¹.

1) Fesenkov Astrophysical Institute, Observatory, 23, Almaty, 050020, Republic of Kazakhstan,
lu.kondr@mail.ru

2) Al-Farabi Kazakh National University, 71 al-Farabi ave., Almaty, 050040 Republic of Kazakhstan

Abstract: In the autumn of 2018, the object V694 Mon underwent the new outburst. It began in only two years after the previous flash in 2016 despite the fact that during the last 25 years the interval between flashes equaled to 1860 days. In the Fesenkov Astrophysical Institute (FAI) of the Republic of Kazakhstan photometric and high resolution spectroscopic observations were carried out since January 25, 2019 till April 14, 2019. Maximal values of brightness $B=9.11\pm 0.01$ mag, $V=8.74\pm 0.01$ mag and $R_c=8.32\pm 0.02$ mag, obtained during this outburst are compared with the maxima of previous flashes. The uniqueness of this active stage is the disappearance of the broad high-velocity absorptions in the profiles of emission lines. These absorptions are formed due to the high collimated jet, flowing out of the white dwarf and directed near to the line of sight. The high-velocity gas of the jet absorbs a continuum in the spectrum of the dwarf or/ and of the red giant. Disappearance of the broad high-velocity absorptions is possible if the inner accretion disk - the source of jet was evacuated during the outburst.

1 Introduction

The peculiar object V694 Monocerotis with the coordinates $\alpha_{2000.0}=07^{\text{h}}25^{\text{m}}51^{\text{s}}$; $\delta_{2000.0}=-07^{\circ}44'08''$ was discovered as a Be star with the bright emission lines by Merrill & Burwell (1943). It consists of a red giant and a white dwarf. There are several estimations of its orbital period: from 1930 to 2000 days (Tomov et al., 1992; Gromadski, Mikolajewska & Whitelock, 2007). Since 1990 this object underwent several outbursts. The last one occurred in the beginning of 2016 (Munari et al., 2016). These authors have analyzed the light curve of V694 Mon from the period 2000-2016 and singled out the five strongest flashes with time interval between them of about 1860 days.

There are emission lines of HI, HeI, and FeII, superimposed on the late-type continuum in the spectrum of V694 Mon. The famous feature of this object is the high collimated jet, flowing out of the white dwarf and directed parallel to the line of sight (Tomov, 1990). It results in the blue-shifted broad absorption components in the emission profiles. In a quiet state the blue edges of absorption components correspond to the velocities between -1600 and -2100 km s⁻¹ (Iijima, 2002; Lucy et al., 2018), and there is a lack of absorption at low velocities. During an active phase, the absorption components can be shifted up to -6500 km s⁻¹ (Tomov, 1990; Schmid et al., 2001).

Table 1: Basic properties of the standard stars

Star	ID	RA[h m s]	DEC[$^{\circ}$:':"]	B	V	$V-R_c$
		2000.0	2000.0	[mag]	[mag]	[mag]
Comp 1	TYC 5396-1090-1	07 25 59	-07 44 12	12.509 ± 0.010	10.784 ± 0.010	
Comp 2	TYC 5396-916-1	07 25 43	-07 42 05	12.359 ± 0.016	11.286 ± 0.016	0.560 ± 0.008
Comp 3	HD 58457	7 25 27.9	-07 44 42	9.780 ± 0.010	8.370 ± 0.010	
Comp 4	TYC 5396-1447-1	07 25 43	-07 47 10	12.442 ± 0.008	11.969 ± 0.008	0.296 ± 0.010
Check 1	TYC 5396-491-1	07 26 00	-07 45 35	10.767 ± 0.006	10.696 ± 0.005	0.032 ± 0.006
Check 2	USNO-B1.0 08222 00179227	07 25 53	-07 42 37	14.035 ± 0.012	12.668 ± 0.010	12.400 ± 0.006

2 Observation and data reduction

The new brightening of the V694 Mon was recorded by Goranskij & Zcharova (2018) and Azzollini & Bellomo (2018) during October - November, 2018. It occurred in two years after the previous flash and, thus, was quite unexpected. Our observations of this active stage were carried out during 80 days, since January 25, 2019 till April 14, 2019.

Photometric observations in BVR_c filters were carried out with the Eastern 1-meter Carl Zeiss Jena telescope located at the Tyan-Shan Observatory of Fesenkov Astrophysical Institute (FAI). Field of view, FOV is $20' \times 20'$, CCD Alta F16M (4096x4096, $9\mu\text{m}$) was used for observations together with the set of BVR_c filters. Each observation consisted of 6-8 exposures in each filter. Exposure times were 40 seconds in the B filter and 10 seconds in the V and R_c filters. Four standard stars from Henden & Munari (2001) were used for calibration. Their characteristics are summarized in Table 1 and they are identified in Figure 1. These stars are well-isolated, with a brightness comparable to the object. As they are located at small angular distance from the target, there is a negligible difference between atmospheric extinction for standards and object. The package MaxIm DL6 was used for data processing. All frames were dark subtracted and flat field corrected. Measurements were derived using a radius aperture of 16 px with local sky readings taken in an annulus of inner radius of 20 px and a width of 14 px. The local BVR_c magnitudes of the object were determined relative to each standard and were transformed to the standard photometric system. The expressions for this procedure were obtained from photometric measurements of the stars from Landolt (2013). The results of the object and standard stars measurements were averaged over all frames received during the night.

The spectroscopic observations were carried out with an Echelle spectrograph mounted on the Western 1-m telescope of Tyan-Shan Observatory. High resolution spectrograms with exposure time of 2400 sec were obtained on January 25, March 13 - 15 and April 14, 2019. Spectrograms were reduced in the standard way using IRAF¹ Echelle package

¹<http://iraf.noao.edu/>

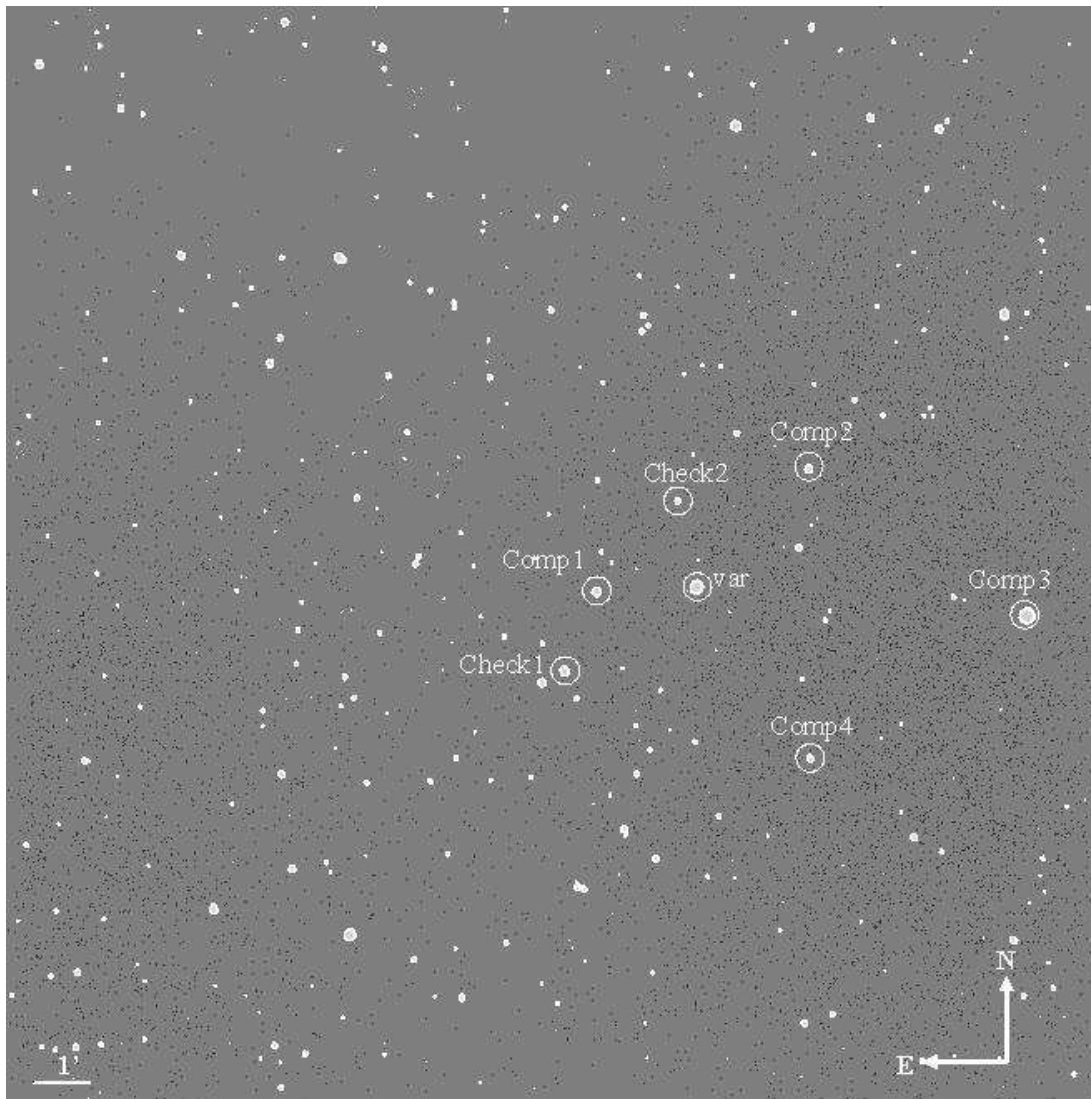


Figure 1: V-band FOV. Positions of the object, comparison and check stars are marked by circles

Table 2: Photometric BVR_c observations of V0694 Mon during the outburst.

Date	JD- 2400000	Phase	B mag	V mag	R_c mag
2019.01.25	58509.22	0.56	9.29±0.02	8.86±0.02	8.31±0.08
2019.03.11	58554.16	0.59	9.38±0.02	8.99±0.01	8.54±0.01
2019.03.14	58557.20	0.59	9.11±0.01	8.74±0.01	8.54±0.01
2019.03.15	58558.13	0.59	9.33±0.01	8.89±0.01	8.38±0.01
2019.03.18	58561.14	0.59	9.33±0.01	8.94±0.01	8.54±0.01
2019.03.20	58563.14	0.59	9.34±0.01	8.87±0.01	8.38±0.01
2019.04.02	58576.16	0.60	9.21±0.01	8.85±0.01	8.32±0.01
2019.04.03	58577.16	0.60	9.39±0.03	8.92±0.01	8.61±0.03
2019.04.14	58588.12	0.61	9.41±0.03	8.89±0.03	8.62±0.02

for subtraction of bias, flat fielding, calibration of the wavelength using Th-Ar lines, normalization of the continuum, and correction to the heliocentric orbit of the Earth. The spectral resolving power $\lambda/\Delta\lambda$ in the range 4300 - 7500 Å is about 50000. The signal to noise ratio SNR in the continuum varies from about 60 at 7400 Å down to about 10 near 4300Å. Outside the specified wavelength range, measurements were not performed due to the high noise level. The output dispersion is 0.08 - 0.11 Å relied on wavelength.

3 Results

The results of our photometric observations are presented in Table 2. Photometric phases were computed according to the ephemeris of Munari et al. (2016):

$$JD_{\max} = 2457460 + 1860 \times E.$$

A plot of our current results together with data obtained in 2010 - 2018 by Munari et al. (2016); Goranskij & Zcharova (2018); Kondratyeva & Rspaev (2012) are presented in Fig 2. Even earlier data can be found for example in (Munari et al., 2016). Two previous flashes took place in 2011-2012 and 2016, the latter being more powerful. Maximal values of BVR_c magnitudes, obtained during the last outburst of 2019 are similar to maximal magnitudes of the flash in 2016.

During the current flash the intensities of emission lines in the spectrum of V694 Mon have increased. The ratios of the maximal line intensities to the level of continuum are plotted in Fig. 3. For comparison we used all results of our long-term observations of this object. It is clear seen that the maximal values of the specified ratios correspond to the maximal brightness of the object in all three filters.

The high resolution profiles of the emission lines $H\gamma$, $H\beta$ and $H\alpha$ are presented in Fig 4. Measurements of the velocities were provided using the laboratory values of wavelengths. Maximal accuracy of the velocity determination is 4-5 km s⁻¹ with the dispersion about 0.1 Å px⁻¹.

Profiles of $H\beta$ and $H\gamma$ obtained on January 25 and March 15, 2019 are quite similar. They are asymmetric with a strong weakening of the blue wings. Red wings extend to velocities 600 - 750 km s⁻¹. Each profile consists of an emission component at the velocity

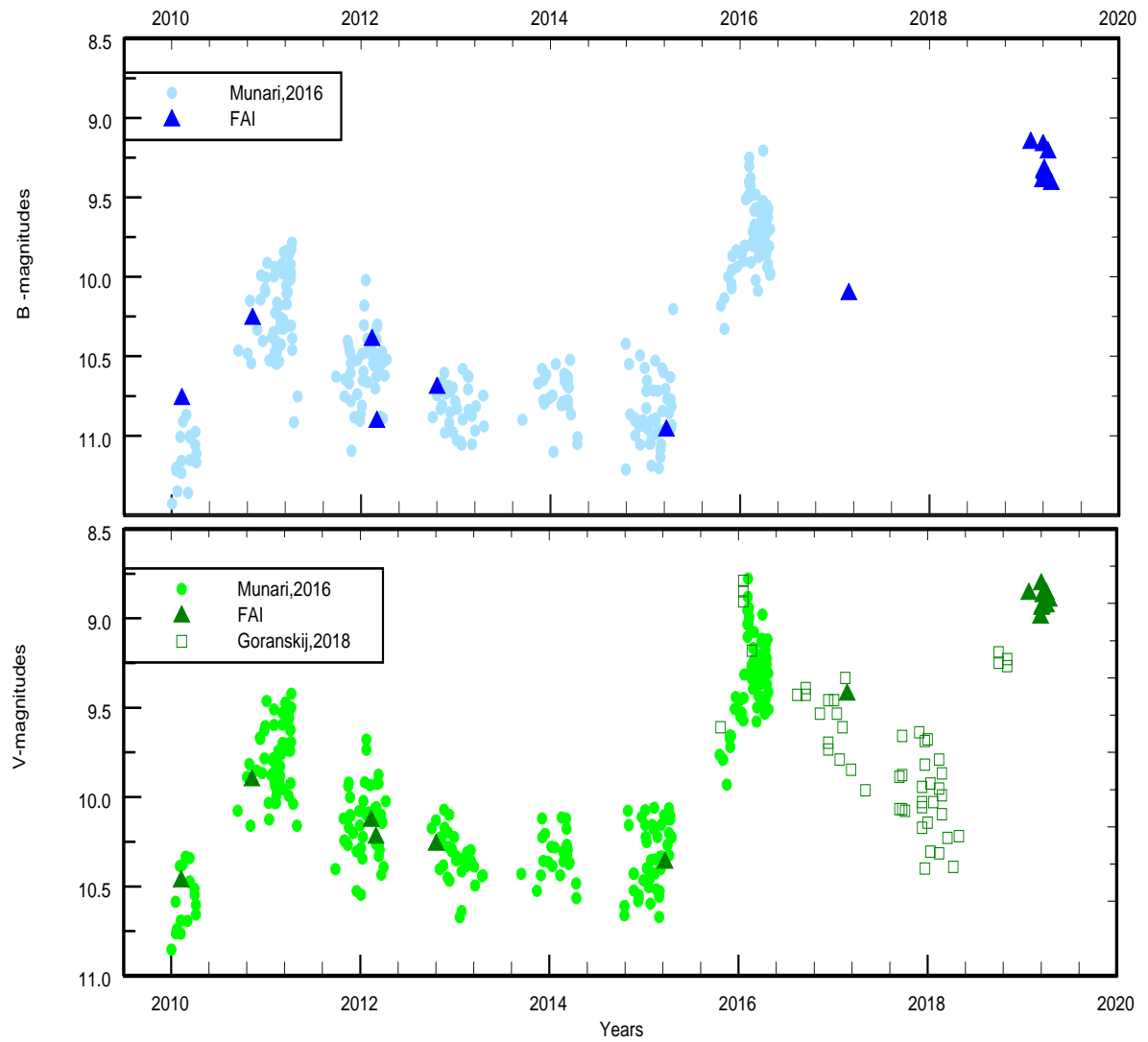


Figure 2: Photometric variations of V694 Mon in the *B* and *V* bands. X-axis shows years, Y-axis gives the magnitudes of the object.

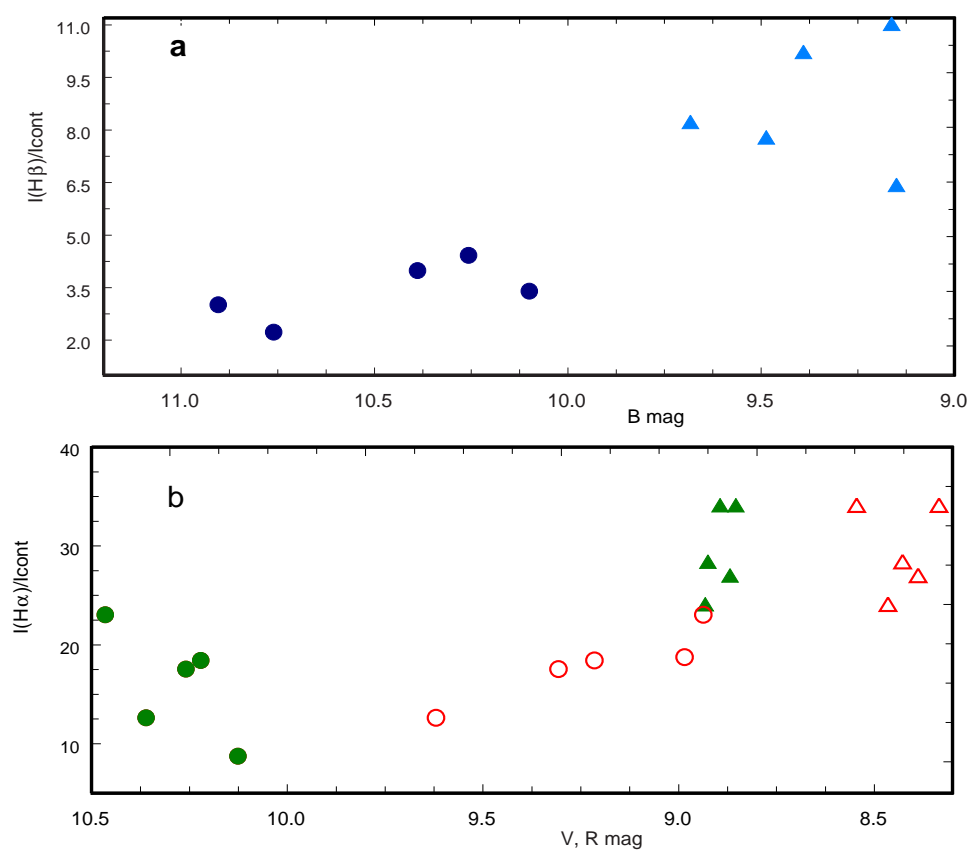


Figure 3: Panel a - dependence of the ratio $I_{\max}(H\beta)/I_{\text{cont}}$ versus the B magnitudes. Panel b - dependence of the ratio $I_{\max}(H\alpha)/I_{\text{cont}}$ versus the V (solid signs) and versus R_c (empty signs) magnitudes. Data obtained in 2019 are marked with the empty and solid triangles.

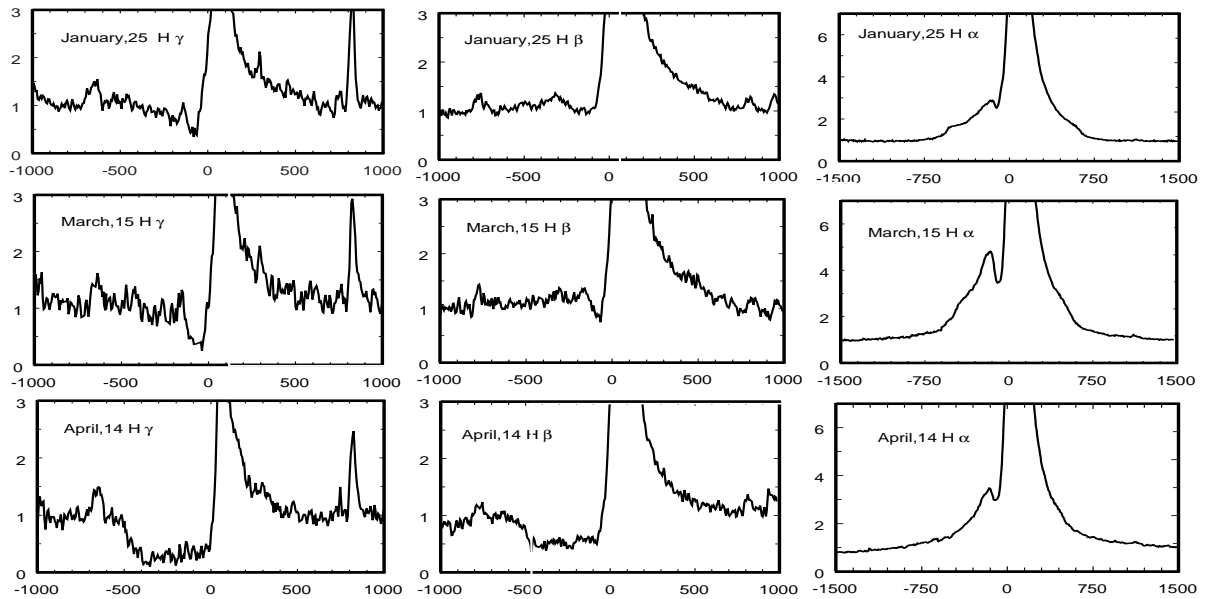


Figure 4: Variation of emission profiles during the current outburst. X-axis shows heliocentric radial velocity (km s^{-1}), Y-axis gives the fluxes normalized to continuum.

$60 \pm 2 \text{ km s}^{-1}$ and a narrow absorption at the $v_r = -70 \pm 5 \text{ km s}^{-1}$. These profiles on the last spectrogram, on April 14 have flat minima spreading from -50 km s^{-1} to about -470 km s^{-1} .

Changes in the $\text{H}\alpha$ profiles are less noticeable, and absorption components are not so deep due to increase of the red giant contribution to the total continuum in this wavelength range. Location of the emission peak also corresponds to $v_r = 60 \pm 2 \text{ km s}^{-1}$. The wings are spreading up to 1100 km s^{-1} in both sides from the line centre. Absorption position is located around the velocity $-105 \pm 5 \text{ km s}^{-1}$. The second emission peaks in the $\text{H}\alpha$ profiles correspond to the velocity -150 km s^{-1} .

Fig 5 presents the profiles of the FeII , 4924 \AA and HeI , 6678 , 7065 \AA lines. The profiles of the FeII lines are similar to the $\text{H}\beta$ and $\text{H}\gamma$ profiles and they change in the same manner. The HeI profiles consist of the traces of emission component and the deep absorption. The HeI profiles obtained on January 25 and March 15 are quite similar. They spread from 0 to about -450 km s^{-1} with the minimum around -150 km s^{-1} . On the last day of observations, the narrow minima are shifted to the bluer wavelength.

For comparison, we present some $\text{H}\beta$ and $\text{H}\alpha$ line profiles obtained in previous years in the quiet period and during the brightening in 2011 (Fig 6) (Kondratyeva & Rspaev, 2012). Spectrograms were obtained with the spectral resolution 0.5 \AA per pixel. It is seen that in almost all panels of Fig 6 the absorption components are located within -700 - -2000 km s^{-1} . The exception is made by profiles received on November 10 and 13, 2010, during the brightening of the object. The blue edges of their absorption components are shifted to about -4000 km s^{-1} .

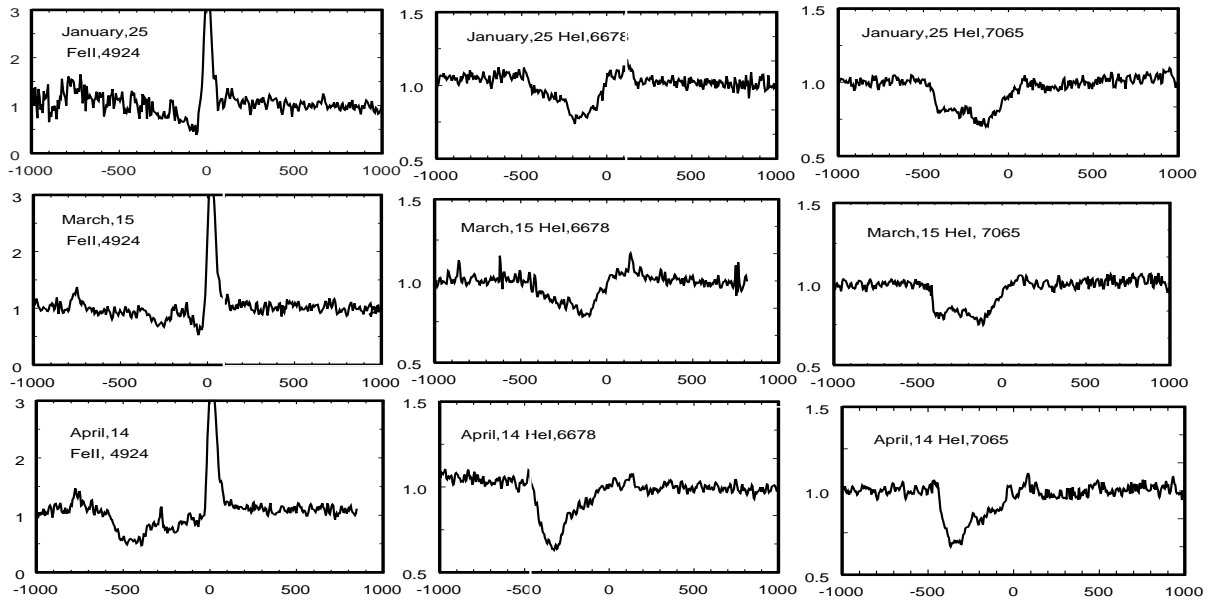


Figure 5: Variation of the FeII and HeI profiles during the current outburst. X-axis shows heliocentric radial velocity (km s^{-1}), Y-axis gives the fluxes normalized to continuum

4 Conclusions

The current outburst of the V694 Mon has been lasting for more than 180 days, if we consider its beginning on October, 2018 (Goranskij & Zcharova, 2018). Maximal values $B = 9.11$ mag and $V = 8.74$ mag were obtained during our observations (Table 2). These results can be compared with data about the previous flashes. The bright active stage in 1990 covered about six months, the maximal brightness $V=9.2$ mag was recorded. Simultaneously the absorption components of HI lines were shifted to -6000 km s^{-1} (Tomov, 1990). During the outburst in 2016 the object has remained around maximum for more than three months, and maximal brightness $B=9.25$ mag, $V=8.78$ mag was obtained (Munari et al., 2016). Thus the 2019 outburst is one of the strongest in the history of V694 Mon.

Munari et al. (2016) found that for a long time from 1990 till 2016 the interval between outbursts was 1860 days. The current flash occurred in the middle of this interval, thus it was quite unexpected.

Since 1990 emission profiles of HI, HeI and FeII lines are accompanied by the broad blue-shifted absorptions owing to the jet. The outflowing collimated gas can create absorption in the continuum of the red giant and of the hot star with its accretion disk. In the quiet phase, the blue edges of a broad absorption were located in the range: $-1500 - -2000 \text{ km s}^{-1}$, during an outburst they were shifted up to -6500 km s^{-1} and there were no traces of absorptions with the lower velocities.

During the current outburst the blue edges of absorptions corresponded to radial ve-

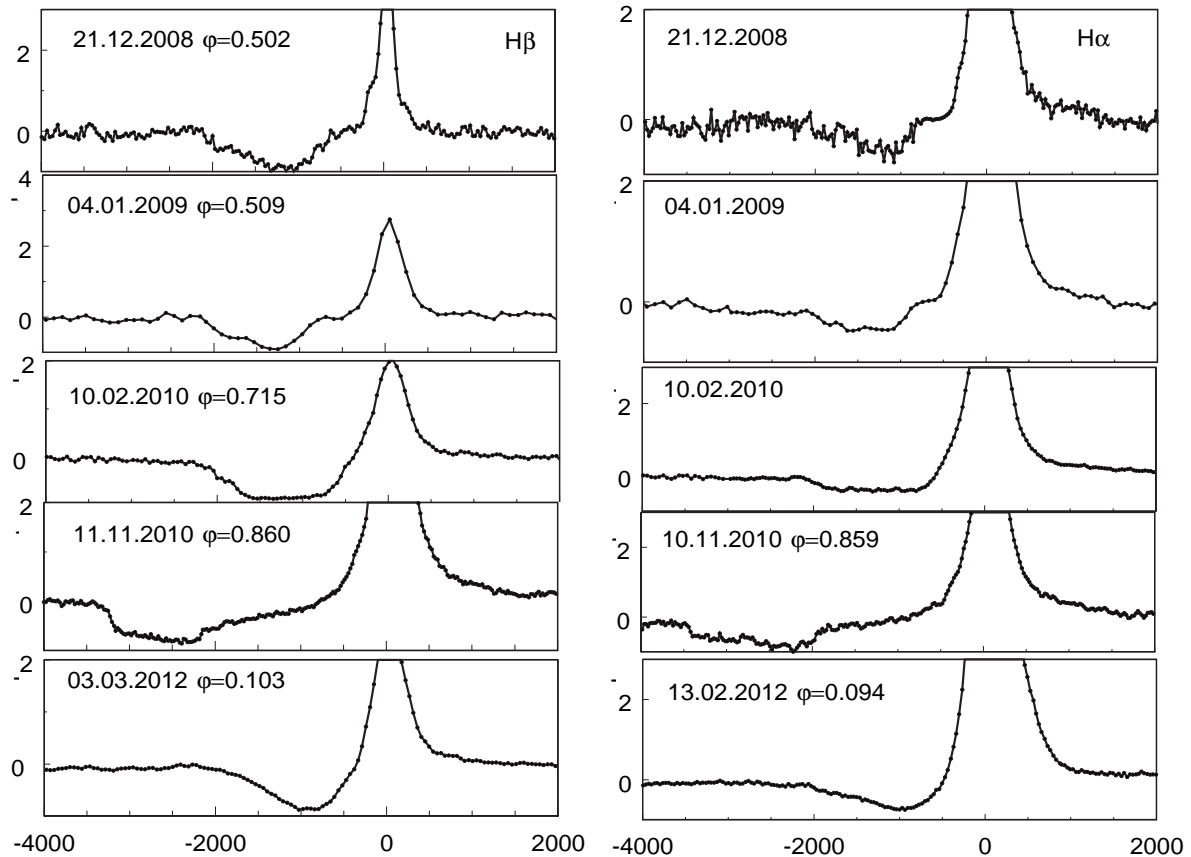


Figure 6: Variation of H β and H α profiles in previous years. X-axis shows heliocentric radial velocity (km s^{-1}), Y-axis gives the ratio $(F(\lambda)-F_{\text{cont}})/F_{\text{cont}}$.

locities $-500 - -600 \text{ km s}^{-1}$, the high-shifted components were not presented at all. This is another distinctive feature of this flash.

Such a flash is usually caused by an increase in the accretion rate of the giant star's matter onto the surface of the accretion disk around the hot component. The accretion disk responds by increasing radiation. As a result, we observe an increase in emission fluxes. However, sometimes during an outburst, evacuation of the inner accretion disk occurs. Jet is formed just in this region, and it vanishes together with its source. It seems that during 2019 outburst we observe just such a case. A similar event occurred in 1990. Then the jet reappeared only in a year, when the inner disk was rebuilt (Lucy et al., 2019).

Acknowledgements: The work was carried out within the framework of Project No. BR05236322, financed by the Ministry of Education and Science of the Republic of Kazakhstan.

References

- Azzollini, A. & Bellomo, M. 2018, *ATel*, No **12231**, 1, [2018ATel....12231....1A](#)
- Goranskij, V. & Zharova, A. 2018, *ATel*, No **12227**, 1, [2018ATel...12227....1G](#)
- Gromadzki, M., Mikolajewska, J., Whitelock, P. 2007, *A&A*, **463**, 703, [2007A&A...463....703G](#)
- Henden, A. & Munari, U. 2001, *A&A* **372**, 145, [2001A&A...372....145H](#)
- Iijima, T. 2002, *A&A*, **391**, 617, [2002A&A...391....617J](#)
- Kondratyeva, L. & Rspaev, F. 2012, *IBVS* **6032**, 1, [2012IBVS...6032....1K](#)
- Landolt, A. 2013, *AJ* **146**, 131, [2013AJ...146....131L](#)
- Lucy, A., Knigge, C. & Sockoloski, J. 2018, *MNRAS* **478**, 568, [2018MNRAS...478....568L](#)
- Lucy, A., Sokoloski, J. & Munari, U. 2019, *arXiv190502399L*, [2019arXiv190502399L...](#)
- Merrill, P. & Burwell, C. 1943, *ApJ*, **98**, 153, [1943ApJ...98....153M](#)
- Munari, U., Dallaporta, S., Castellani, F., et al. 2016, *New Astronomy*, **49**, 43, [2016NewAstr....49....43M](#)
- Schmid, H., Kaufer, A., Camenzind, M., et al. 2001, *A&A* **377**, 206, [2001A&A...377....206S](#)
- Tomov, T. 1990, *IAUC* **4955**, 1, [1990IAUS....4955....1T](#)
- Tomov, T., Kolev, D., Ivanov, M., et al. 1992, *A&AS* **116**, 1, [1992A&AS....116....1T](#)